Available online at www.sciencedirect.com
ScienceDirect
Journal of Molecular Catalysis A: Chemical 278 (2007) 181–188
JOURNAL OF MOLECULAR CATALYSIS A: CHEMICAL
www.elsevier.com/locate/molcata

On the mechanism of the catalytic destruction of 1,2-dichloroethane over Ce/Zr mixed oxide catalysts

Beatriz de Rivas, Rubén López-Fonseca, Juan R. González-Velasco, José I. Gutiérrez-Ortiz *

Chemical Technologies for Environmental Sustainability Group, Department of Chemical Engineering, Faculty of Science and Technology, Universidad del País Vasco/EHU, P.O. Box 644, E-48080 Bilbao, Spain

Received 11 July 2007; received in revised form 4 September 2007; accepted 4 September 2007
Available online 8 September 2007

Abstract

This study has been undertaken to investigate the efficiency of ceria, zirconia, and $Ce_xZr_{1-x}O_2$ mixed oxides as catalysts for the 1,2-dichloroethane destruction in dry air. Mixed oxides exhibit promoted redox and acidic properties, which result catalytically relevant for the oxidation of this chlorinated compound. Considering all compositions it was observed that catalytic activity varies as a function of zirconia content, being $Ce_{0.5}Zr_{0.5}O_2$ the sample which showed a better performance. The notable improvement in catalyst activity of CeO_2 can be achieved through structural doping with Zr ions.

Likewise, the present study has been focused on the elucidation of the pathway involved in the progressive oxidation of the chlorinated hydrocarbon as a function of the temperature by means of FTIR. It is postulated that the destruction of 1,2-dichloroethane at low temperatures proceeds through dehydrochlorination into vinyl chloride in the presence of acid sites. This compound can be protonated in the presence of OH surface species forming carbonium ions that can be attacked by nucleophilic oxygen species from the catalyst to form chlorinated alkoxide species. These intermediates readily decompose to generate acetaldehyde, which can be further oxidised into acetates and finally degraded to CO_x.

Keywords: Catalytic combustion; Ceria–zirconia mixed oxides; 1,2-Dichloroethane; IR-spectroscopy; Oxidation mechanism

1. Introduction

Volatile organic compounds are considered as one of the main air pollutants, either directly through their toxic or malodorous nature, or indirectly as ozone precursors and smog precursors. Besides main emission sources such as petroleum industries, there are a lot of local sources such as painting, printing and laundry which emit VOCs stream of low concentration. Among all VOCs, chlorine-containing compounds require a special attention due to their toxicity, high stability and widespread application in industry [1].

The noxious effect on the environment makes their removal imperative. Thus, the environmental legislation has already established in many countries severe regulations for the control of VOCs emissions. Particularly, the Gothenburg Protocol adopted by the 15 EU member states in 1999 requires a 40% reduction in VOCs emissions by 2010. In view of the scale of the problem presented to the chemical and processing industries the major challenge they face is to reduce the emission of polluting VOCs with minimal economic impact. Thus, complete elimination or, at least, abatement below the levels fixed by environmental regulations is a major concern in developed countries.

The satisfaction of stringent standards on VOCs emissions requires significant improvement of the efficiency of VOCs removal technologies. In the last years the reduction of their atmospheric concentration by means of preventive catalytic combustion has acquired great importance owing to its ability to destroy these pollutants at a far lower temperature than those required for thermal destruction [2]. As a consequence there is no associated pollution by dioxins and nitrogen oxides (NO_x), as they are usually formed under high temperature condition. Furthermore, catalytic deep oxidation is more selective and as it requires less heating, is more cost effective. However, because

* Corresponding author. Tel.: +34 94 6012683; fax: +34 94 6015963.
E-mail address: joseignacio.gutierrez@ehu.es (J.I. Gutiérrez-Ortiz).

1381-1169/$ – see front matter © 2007 Elsevier B.V. All rights reserved.
doi:10.1016/j.molcata.2007.09.006

large gas volumes have to be treated, this has to be performed at very high space velocity and thus requires very highly active catalysts.

The development of new catalysts for low temperature complete oxidation of VOCs to produce CO_2 (and HCl for chlorinated VOCs) is a subject of continuous interest. Numerous materials have been evaluated as catalysts for oxidising hydrocarbons and chlorocarbons [3–5]. These materials are usually divided into noble metal-based materials and transition metal oxides. Although supported noble metals are preferred in general due to their high activity, the efficiency of a catalyst depends to a greater extent on the nature of the VOCs to be combusted and the catalyst behaviour cannot be predicted a priori. This is illustrated by the fact that some metal oxides can be more active than noble metals [6]. In addition, noble metals are more expensive and less resistant to poisoning.

Over the past several years cerium oxide and CeO_2-containing materials have come under intense scrutiny as catalysts and as structural and electronic promoters of heterogeneous catalytic reactions. Concretely, CeO_2 and CeO_2 structurally doped with Zr oxides have attracted much attention as oxidation catalyst because of their unique redox properties and high oxygen storage capacity [7,8]. The utilisation of this type of oxides as a key component in three-way catalysts for the treatment of exhaust gas from automobiles constitutes its most important applications from the economic and technological points of view [9,10]. However, other environmental catalytic applications have been reported. For instance, ceria has potential uses for the removal of post-combustion pollutants and of recalcitrant organics from wastewater [11–14]. Nevertheless, little attention has been focused on investigating ceria–zirconia mixed oxides as potential catalysts for the efficient removal of chlorinated organic pollutants from waste gas streams by low temperature combustion.

This paper is specifically devoted to the analysis of the reaction mechanism of the oxidative 1,2-dichloroethane over Ce/Zr mixed oxides by means of a combined flow and infrared spectroscopy study. IR can result in a useful technique for obtaining direct evidence of the presence and nature of surface intermediates leading to a better understanding of the progressive catalytic oxidation of DCE. Up to now, only a few papers have discussed the reaction mechanism of the oxidation of chlorinated compounds oxidation [15–17].

2. Experimental

2.1. Catalyst preparation

Ceria–zirconia mixed oxides ($Ce_xZr_{1-x}O_2$) with varying molar composition ($x = 0.15$, 0.5, 0.68 or 0.8) were synthesised by Rhodia using a precipitation route from nitrate precursors. Rhodia also provided the pure ceria sample whereas the pure zirconia sample was supplied from Norton. All oxides were stabilised by calcination in air at 550 °C for 4 h. Catalyst pellets with diameter from 0.3 to 0.5 mm were prepared by compressing the oxide powders into flakes by means of an hydraulic press, followed by crushing and sieving.

2.2. Catalyst characterisation

Textural properties were determined by multi-point N_2 adsorption–desorption at −196 °C using an automatic Micromeritics ASAP 2010 equipment. Data were treated in accordance with the BET and BJH methods. The samples were previously degassed overnight at 300 °C under high vacuum. X-ray diffraction (XRD) studies were carried out on a X'PERT-MPD X-ray diffractometer with Cu Kα radiation ($\lambda = 1.5406$ Å) and Ni filter. The X-ray tube was operated at 30 kV and 20 mA. Samples were scanned from $20° < 2\theta < 80°$ and the X-ray diffraction line positions were determined with a step size of 0.02° and a counting time of 2.5 s per step. Indexation and calculation of unit cell parameters were carried out by using the intensities of lines (1 1 1) of CeO_2 and $Ce_xZr_{1-x}O_2$ ($x > 0.5$) (cubic structure), (1 0 1) of $Ce_xZr_{1-x}O_2$ ($x \leq 0.5$) (tetragonal structure), and (1 1 1) and (1 0 1) of ZrO_2 (monoclinic structure).

Temperature-programmed desorption (TPD) of NH_3 was performed on a Micromeritics AutoChem 2910 instrument equipped with a thermal conductivity detector (TCD). Prior to adsorption experiments, the samples (20 mg) were first pretreated in a quartz U-tube in a 5%O_2/He stream at 550 °C. Then, they were cooled down at 100 °C in an He flow (20 $cm^3\ min^{-1}$) before the adsorption of the probe molecule started. The amount of gases desorbed was determined by time integration of the TPD-curves. The NH_3 adsorption step was performed by admitting small pulses of ammonia in He at 100 °C up to saturation. Subsequently, the samples were exposed to a flow of helium (50 $cm^3\ min^{-1}$) for 2 h at 100 °C in order to remove reversibly and physically bound ammonia from the surface. Finally, desorption was carried out from 100 to 550 °C at a heating rate of 10 °C min^{-1} in an He stream (50 $cm^3\ min^{-1}$). This temperature was maintained for 120 min until the adsorbate was completely desorbed.

Diffuse reflectance infrared Fourier-transform spectra (DRIFTS) of adsorbed pyridine adsorbed on the catalysts were recorded with a Nicolet Protegé 460 ESP spectrometer equipped with a controlled-temperature and environment diffusive reflectance chamber (Spectra-Tech) with KBr windows and a liquid nitrogen-cooled HgCdTe detector. All spectra were collected in the range of 4000–800 cm^{-1} averaging 400 scans at an instrument resolution of 1 cm^{-1}. The spectra were analysed using OMNIC software. Prior to pyridine adsorption the sample was evacuated at 550 °C and 1.33×10^{-3} N m^{-2} for 1 h, and cooled to 50 °C. Consequently, pyridine vapour doses were injected by syringe through a septum until the sample was saturated. Spectra were recorded at 200 °C after 1 h under vacuum in order to reduce the contribution of the gas phase and physisorbed pyridine. Difference spectra were obtained by subtracting the spectrum of the clean sample from the spectra obtained after pyridine adsorption.

The redox behaviour was examined by temperature-programmed reduction and oxygen storage capacity experiments. Temperature-programmed reduction (TPR) experiments were conducted on a Micromeritics AutoChem 2910 instrument as well. First, all samples were pre-treated in an oxygen stream

(5%O_2/He) at 550 °C for 1 h, and then cooled down to room temperature. The reducing gas used in all experiments was 5%H_2 in Ar, with a flow rate of 50 cm^3 min^{-1}. The temperature range explored was from room temperature to 950 °C with a heating rate of 10 °C min^{-1}. The water produced by reduction was trapped into a cold trap. The consumption of H_2 was quantitatively measured by time integration of the TPR-profiles. Oxygen storage capacity (OSC) measurements were carried out on a Micromeritics ASAP 2010 equipment. In order to clean the surface, the samples were first calcined at 550 °C for 1 h in a 5%O_2/He stream. Then, the sample was subjected to a reduction treatment with a pure hydrogen stream at 550 °C. Finally, the measurement of oxygen consumption (5%O_2/He) at 400 °C was evaluated.

2.3. Experimental set-up and procedure

Catalyst behaviour was determined using a lab-scale fixed-bed reactor, in which typically 0.85 g of catalyst was loaded. Catalysts were tested in powdered form (0.3–0.5 mm) using a 12-mm i.d. stainless-steel reactor tube [18]. The reaction feed consisted of 1000 ppm of DCE in dry air. The feed stream to the reactor was prepared by delivering the liquid hydrocarbon by a syringe pump (Cole Palmer 74900-00) into dry air, which was metered by a mass flow controller (Brooks). A total flow rate of 500 cm^3 min^{-1} was used and catalysts were packed to a constant volume to give a gas hourly space velocity of 30,000 h^{-1}. Catalytic activity was measured over the range 200–550 °C, and temperatures were measured by a thermocouple placed in the catalyst bed. Conversion data were calculated by the difference between inlet and outlet concentrations. Conversion measurements and product profiles were taken at steady state, typically after 30 min on stream. Either product selectivity was calculated based on either chlorine or carbon atoms present in that product divided by the total chlorine or carbon atoms present in the product stream (expressed as %).

The feed and effluent streams were analysed using an on-line gas chromatograph (Hewlett Packard 5890 Series II) equipped with a thermal conductivity detector (CO and CO_2) and an electron capture detector (chlorinated hydrocarbons). Analysis of HCl and Cl_2 was carried out by means of ion selective electrode and titration, respectively. Further details on analytical procedures are given elsewhere [18].

The adsorption and subsequent decomposition of DCE was studied by Fourier transform infrared spectroscopy (FTIR). All spectra were recorded at 100 °C on a Nicolet Protegé 460 ESP spectrometer equipped with a DTGS detector averaging 100 scans with a 1 cm^{-1} resolution and analysed using OMNIC programme software. About 50 mg of the catalyst were pelleted as a disc 13 mm in diameter. The spectra were taken in a device which consisted of a cell (SpectraTech) with ZnSe windows. The catalyst was pre-treated by heating at 550 °C for 1 h in a mixture of N_2 (200 ml min^{-1}) and O_2 (50 ml min^{-1}). The spectrum recorded at 100 °C after the thermal treatment was used for substraction as a blank. Next, a gas stream containing 1000 ppm DCE (DCE/O_2/N_2) was introduced into the cell at 100 °C for 20 min. The stream was prepared by delivering the liquid compound by a syringe pump (Cole Palmer 74900-00) into the flowing O_2/N_2 mixture (20%). Before entering the cell, the feed stream was homogeneously blended in a 1 dm^3 static mixer, which served to dampen out possible oscillations of the syringe pump as well. Next, the cell was purged at 100 °C for 30 min under N_2 atmosphere to remove the gas phase species. Then, the spectrum was recorded. Afterwards, the sample was heated up to 200 °C and the DCE/O_2/N_2 stream was again re-introduced into the cell for 20 min. After evacuation with N_2 and cooling (100 °C) the spectrum was taken. This experimental procedure was repeated at 300 °C. In this way, possible transformations of the adsorbed species were recorded at a series of increasing temperatures. All gases were delivered to the sample at atmospheric pressure. The flow rate of each gas was controlled by a mass flow controller (Bronkhorst). Circulating water was used to cool the body of the reaction cell. The temperature was controlled by a thermocouple in direct contact with the sample.

3. Results and discussion

3.1. Physico-chemical characterisation

Results from physico-chemical characterisation are given in detail elsewhere [19]. Hence, the most relevant properties of the catalysts are summarised in Table 1. All cerium-containing samples showed a surface area of about 100 m^2 g^{-1}, except for the $Ce_{0.15}Zr_{0.85}O_2$ sample (85 m^2 g^{-1}). The structural properties appeared to depend on the cerium content. Thus, samples with molar cerium content higher than 68% exhibited a cubic structure whereas a tetragonal structure was evidenced for mixed oxides with a lower cerium content (50% and 15%). On the contrary, the structure of the pure zirconia sample was monoclinic. The cell parameter (a_0) for the $Ce_xZr_{1-x}O_2$ mixed oxides calculated from the main diffraction peaks displayed a linear decrease of a_0 with increasing ZrO_2 content, in agreement with the Vegard rule since the Zr^{4+} ionic radius (0.084 nm) is smaller than that of Ce^{4+} (0.098 nm) [20].

Acid sites play an important role in the adsorption and reaction of different type of hydrocarbons on the surfaces of ceria-based materials. TPD of ammonia allowed to evaluate the acidic properties of the different samples. It is widely known that chemical mixing with another oxide can significantly change the acid properties of a given metal oxide. Indeed, the incorporation of increasing quantities of zirconium into the ceria lattice led to marked increase in the total and strong acidity (Table 1). Therefore, the highest and strongest acidity was found for the $Ce_{0.15}Zr_{0.85}O_2$ mixed oxide [19]. On the other hand, pyridine adsorption followed by DRIFTS was carried out in an attempt to determine the nature of the acid sites discriminating between Brønsted and Lewis. Fig. 1 shows the infrared spectra of pyridine adsorbed on Ce/Zr mixed oxides at 200 °C in the region between 1700 and 1400 cm^{-1}. Lewis acid sites (1450 cm^{-1}) and H-bond donor sites (1540 cm^{-1}) were found on all the oxides. The former type of site was associated with coordinatively unsaturated metal ions, whereas the latter type was related to partially positively charged surface OH groups. The surface of ZrO_2 and the oxide with the largest amount of Zr were shown to be unique in

Table 1
Main physico-chemical properties of $Ce_xZr_{1-x}O_2$ catalysts

Catalyst	BET surface area ($m^2\,g^{-1}$)	Pore volume ($cm^3\,g^{-1}$)	Average pore size (Å)	Structure	Lattice parameter (Å)	Total acidity ($mmol\,NH_3\,g^{-1}$)	Strong sites ($mmol\,NH_3\,g^{-1}$)	H_2 consumption ($mmol\,g^{-1}$)	Oxygen adsorption capacity ($mmol\,g^{-1}$)
CeO_2	99	0.21	59	Cubic	5.41	0.14	0.09	0.20	0.05
$Ce_{0.8}Zr_{0.2}O_2$	102	0.18	48	Cubic	5.35	0.17	0.08	1.00	0.32
$Ce_{0.68}Zr_{0.32}O_2$	101	0.24	70	Cubic	5.30	0.22	0.12	1.29	0.41
$Ce_{0.50}Zr_{0.50}O_2$	99	0.21	64	Tetragonal	5.26	0.35	0.24	1.32	0.45
$Ce_{0.15}Zr_{0.85}O_2$	86	0.28	102	Tetragonal	5.14	0.41	0.31	0.51	0.18
ZrO_2	51	0.25	157	Monoclinic	–	0.31	0.24	–	–

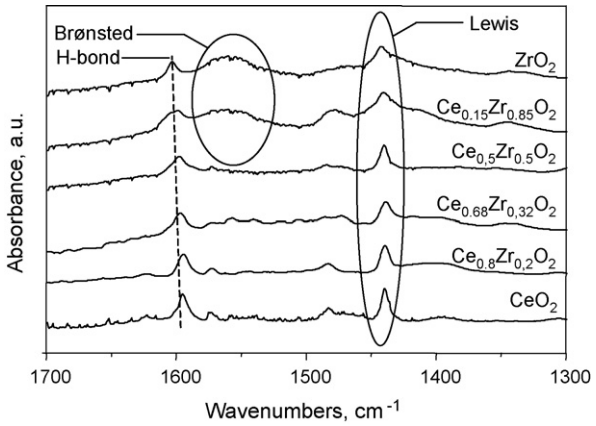

Fig. 1. IR spectra of adsorbed pyridine on $Ce_xZr_{1-x}O_2$ catalysts after adsorption and desorption at 200 °C.

exposing Brønsted acid sites, as identified by the formation of BPy species.

On the other hand, the redox properties of ceria-containing materials were investigated by temperature-programmed reduction performed with hydrogen and by measuring oxygen storage capacity. The redox process was found to be promoted in the mixed oxides with respect to the pure cerium oxide. Thus, insertion of ZrO_2 into the cubic CeO_2 resulted in a distortion on the mixed oxide which led to a higher mobility of the lattice oxygen, and consequently the reduction was no longer confined to the surface but extended deep into the bulk [21]. Thus, it was noted that the extent of the reduction and oxygen consumption was larger for the $Ce_{0.5}Zr_{0.5}O_2$ sample. Since the charge/radius of Ce^{3+} (radius 0.114 nm) is significantly lower than that of Ce^{4+} (radius 0.097 nm), the formation of vacancies or structural defects was promoted, and as a result the oxygen mobility was favoured [22].

3.2. Catalytic performance and product selectivity of DCE decomposition

The destruction of DCE over Ce/Zr oxides was examined by means of the corresponding ignition or light-off curves, characterised by the T_{50} parameter (temperature needed to attain 50% conversion) (Table 2). Note that these results are described in detail in elsewhere [19]. Briefly, a noticeable catalytic performance was observed for the CeO_2 and the mixed oxide catalysts, as revealed by the low temperatures required for the deep decomposition of the chlorinated compound. In this sense,

Table 2
T_{50} values (°C) and peak concentration values (ppm) of VC at 400 °C over $Ce_xZr_{1-x}O_2$ catalysts in the oxidation of DCE

	T_{50}	VC
CeO_2	320	200
$Ce_{0.8}Zr_{0.2}O_2$	310	175
$Ce_{0.68}Zr_{0.32}O_2$	305	165
$Ce_{0.50}Zr_{0.50}O_2$	295	145
$Ce_{0.15}Zr_{0.85}O_2$	315	200
ZrO_2	360	555

it was observed that the mixed oxide with an equimolar composition, $Ce_{0.5}Zr_{0.5}O_2$, showed the highest activity. This result highlighted the beneficial synergy that could be achieved by structural doping CeO_2 by ZrO_2. Hence, the higher activity observed with respect to the pure oxides was associated with a suitable combination of surface acidity with relatively accessible lattice oxygen species. Accordingly, it is suggested that the first stage of the oxidation process is the adsorption of the chlorinated molecule on an acid site [19], which subsequently could be attacked by mobile oxygen species from the solid solution through a Mars-van Krevelen mechanism [23].

The function of surface acidity in chlorocarbon destruction was consistent with previous reports on different types of catalysts such as zeolites [24,25], alumina [26], TiO_2/SiO_2 [27], ZrO_2/SO_4 [28], or TiO_2/ZrO_2 [29]. Likewise, the catalytic role of acid sites has been reported for ceria–zirconia catalysts as well [30,31]. These studies point out that the promoting effect of acid sites was basically related to the composition of the mixed oxide [32,33]. Additional experiments carried out in the absence of oxygen in the feed stream revealed the key role played by oxygen species from the catalyst as a significant activity of mixed oxides was found under these conditions [19].

As far as product selectivity was concerned, CO, CO_2, HCl and Cl_2 were the major products obtained during the oxidation of DCE. Besides, significant amounts of vinyl chloride (VC), 115–300 ppm, were identified at mild temperatures (250–450 °C) as a chlorinated intermediate (Table 2). This by-product was presumably formed by dehydrochlorination of DCE, and completely oxidised at high temperatures [19].

The evolution of the selectivity towards HCl, the preferred chlorinated oxidative product, over various catalysts as a function of temperature is shown in Fig. 2. HCl profile revealed a first drop with the temperature up to around 400 °C. This fact could be explained by the formation of VC and Cl_2. As stated above, the presence of notable amounts of VC suggested that the abstraction of HCl was the first step in the reaction process. VC peak concentration varied as a function of catalyst composition (Table 2). It is worth pointing out that ceria–zirconia mixed oxides gave rise to considerably lower quantities (145–200 ppm) of this intermediate than pure zirconia (555 ppm), and to slightly lower quantities compared with pure ceria (200 ppm). This result was in agreement with the fact that VC generation was closely associated with the acid properties of the oxides. However, the pure zirconia, an acid catalyst with negligible redox properties, was found to yield the largest amount of VC in spite of its moderate acidity. Conversely, mixed oxides, which exhibit a varying combination of acid and redox properties as a function of their Ce/Zr molar ratio, limited the formation of this compound. In this way, it was proposed that the promoted redox properties favoured the decomposition of this intermediate. At temperatures above 400 °C the increasing concentration of HCl, which led to higher HCl selectivity values, resulted from an enhanced conversion of DCE and VC, while the observed chlorine generation was exclusively assigned to the occurrence of the oxidation of HCl according to the so-called Deacon reaction ($2HCl + O_2 \leftrightarrow Cl_2 + H_2O$). Note that DCE contains sufficient hydrogen for the complete oxidation to HCl. The extent of this reaction was promoted as the cerium content in the solid solution increased. Hence, selectivity to Cl_2 at 550 °C increased from 4% over ZrO_2 to 40% over CeO_2.

In addition to chlorinated reaction products, carbon dioxide was found to be the major non-chlorinated reaction product. Nevertheless, CO was also observed in the 250–450 °C temperature range but as reaction temperature increased lower concentrations were detected. Hence, the CO_2 selectivity values were in the order of 70–95% over mixed oxides and pure ceria. The CO/CO_2 ratio was found to be the lowest for CeO_2. It is highly accepted that CeO_2 in its pure form is a complete oxidation catalyst [31]. Conversely, pure zirconia, which is a relatively poor deep oxidation catalyst, gave rise to significant amounts to carbon monoxide (70% CO_2 selectivity) [19].

3.3. DCE decomposition followed by FTIR

In situ decomposition of 1,2-dichloroethane was investigated at three different temperatures, viz., 100, 200 and 300 °C by FTIR to aid in detecting all the possible intermediates (which

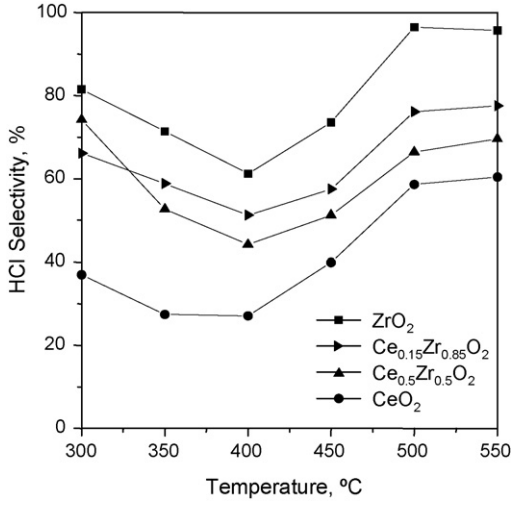

Fig. 2. Selectivity values (%) to HCl over $Ce_xZr_{1-x}O_2$ catalysts in the oxidation of DCE.

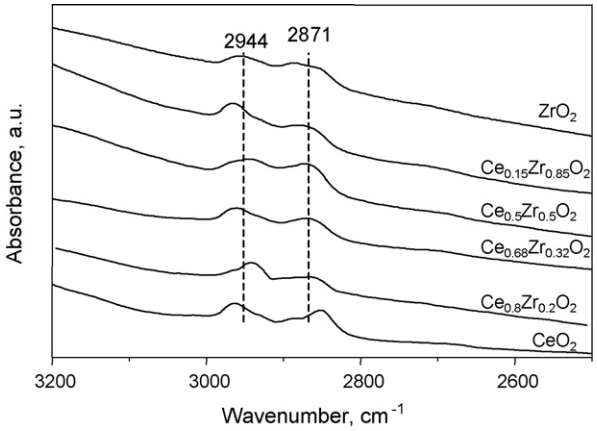

Fig. 3. C–H stretch vibration for adsorption of DCE on $Ce_xZr_{1-x}O_2$ at 100 °C.

Table 3
Absorption bands for adsorption of DCE on $Ce_xZr_{1-x}O_2$ catalysts at 100 °C

	Gas phase	CeO_2	$Ce_{0.5}Zr_{0.5}O_2$	ZrO_2
$\nu_{as}(CH_2)$	2976	2968	2944	2955
$\nu_s(CH_2)$	2888	2852	2872	2880
$\rho(CH_2)$	1238	1233	1236	1235

might not otherwise be visible at high temperature) leading to the formation of complete oxidation products. Fig. 3 displays the C–H stretching frequency range for the decomposition of DCE on $Ce_xZr_{1-x}O_2$ oxides at 100 °C. The two main bands located at around 2950 and 2870 cm^{-1}, depending on the catalyst composition, were respectively assigned to asymmetric $\nu_a(CH_2)$ and symmetric $\nu_s(CH_2)$ stretching vibrations [15]. The presence of these bands evidenced that the DCE adsorption on the surface of Ce/Zr catalyst is the first step of the reaction mechanism. An slight shift of the band positions with respect to the modes of vibration in the gas phase (Table 3) was noticed.

Additionally, Fig. 4 shows the evolution of the absorption IR bands as a function of the temperature on $Ce_{0.5}Zr_{0.5}O_2$ sample, the most active catalyst, in the range between 4000 and 2000 cm^{-1}. The spectrum corresponding to the fresh sample was also included for the sake of comparison. As aforementioned, the presence of the IR bands characteristic of CH_2 group vibrations evidenced the adsorption over the surface catalyst. As the temperature increased, these bands were slightly shifted towards higher wavenumbers, reaching a maximum intensity at 200 °C. On the other hand, the presence of a wide band at around 3440 cm^{-1}, attributed to the progressive water formation due to DCE decomposition with increasing temperature, was clearly observed as well [35]. The partial conversion of the feed was also assessed by the detection of a weak doublet at 2358 and 2323 cm^{-1}, which was assigned to adsorbed CO_2 [36,37] (graph on the right top of Fig. 4).

The interpretation of the infrared spectra in the region between 1800 and 800 cm^{-1} resulted significantly more difficult owing to the presence of several bands. Fig. 5 shows the infrared spectra recorded at different temperatures on $Ce_{0.5}Zr_{0.5}O_2$, which are characterised by a series of bands located at 1598, 1560, 1450, 1367, 1294, 1236, 1070, 1025, 941 and 893 cm^{-1}. Based on the literature frequencies and assignments (Table 4), the set of bands constituted by 1598 cm^{-1} ν(C=C), 1294 cm^{-1} ρ(C–H), 1025 cm^{-1} $\rho(CH_2)$, 941 cm^{-1} $\delta(CH_2)$ and 893 cm^{-1} δ(C–Cl) corresponded to vinyl chloride formation over the catalytic surface [15,16]. Note that these bands are marked with italic characters in Fig. 5 (also in Figs. 6–8). It is worth pointing out that the generation of this intermediate was consistent with the flow experiments.

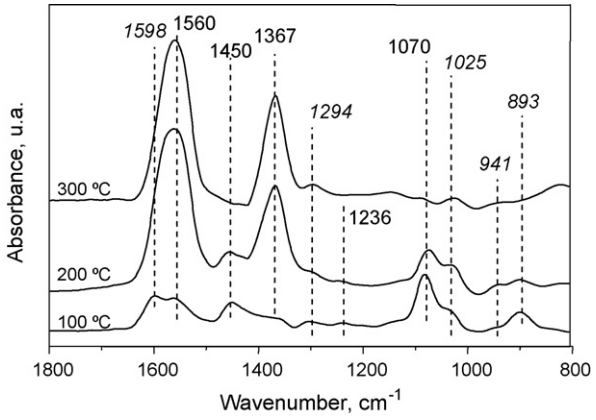

Fig. 5. Infrared spectra of DCE decomposition on $Ce_{0.5}Zr_{0.5}O_2$ catalyst at different temperatures (1800–800 cm^{-1}).

Table 4
Absorption bands of adsorbed VC on $Ce_xZr_{1-x}O_2$ catalysts

	Gas phase	CeO_2	$Ce_{0.5}Zr_{0.5}O_2$	ZrO_2
ν(C=C)	1599	1599	1598	1604
ρ(C–H)	1290	1284	1294	1298
$\rho(CH_2)$	1023	1028	1025	1018
$\delta(CH_2)$	941	943	946	950
δ(C–Cl)	897	887	893	897

Further, a comparative analysis of the bands corresponding to VC adsorbed at 100 °C on the catalyst surface of various catalysts (CeO_2, ZrO_2 and $Ce_{0.5}Zr_{0.5}O_2$) indicated that this molecule was formed in relatively low quantities over the zirconia catalyst (its formation required higher temperatures). However, VC was

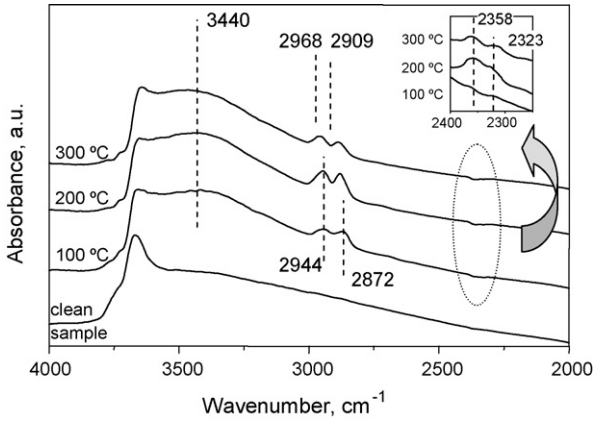

Fig. 4. Infrared spectra of DCE decomposition on $Ce_{0.5}Zr_{0.5}O_2$ catalyst at different temperatures (4000–2000 cm^{-1}).

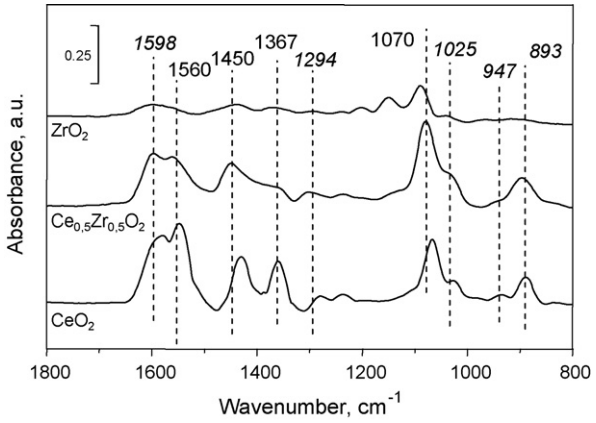

Fig. 6. Infrared spectra of DCE decomposition on $Ce_xZr_{1-x}O_2$ catalysts at 100 °C (1800–800 cm^{-1}).

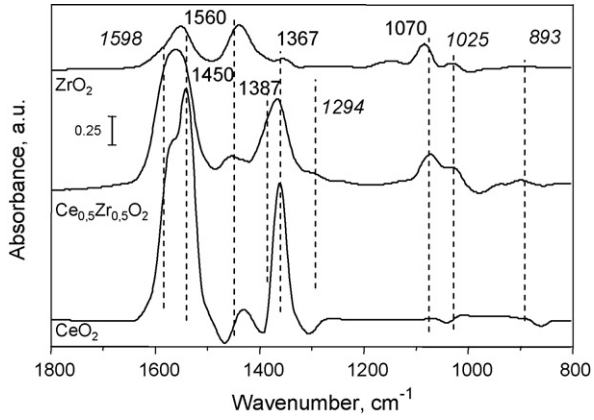

Fig. 7. Infrared spectra of DCE decomposition on $Ce_xZr_{1-x}O_2$ catalysts at 200 °C (1800–800 cm^{-1}).

found to be more abundant over CeO_2 and $Ce_{0.5}Zr_{0.5}O_2$ (Fig. 6). On the other hand, as suggested by the disappearance of the IR bands, this compound was converted to a major extent as the temperature increased (Figs. 7 and 8). This was again in agreement with the flow experiments, where VC was not observed as a reaction product at higher temperatures.

In addition, the band centered at 1070 cm^{-1} can be due to ν(C–O) vibration of methoxy species [38,39]. The absorption bands at 1560 and 1450 cm^{-1} represent asymmetric stretching and symmetric stretching, respectively, of the carboxylate $\nu(COO^-)$ of the acetate type [15,40,41], whereas the band 1367 cm^{-1} was assigned to the deformation of CH_3 group, $\delta(CH_3)$ [17,42]. As a consequence, it could be deduced that the reaction, after the adsorption of the compound and formation of VC, involved the formation of intermediate oxygenated species such as alkoxides and acetates. These groups were more visible over CeO_2 and $Ce_{0.5}Zr_{0.5}O_2$ oxides and with increasing temperature (Figs. 6–8). At higher temperatures these oxygen containing species underwent further oxidation to yield complete oxidation products (Fig. 4). The absence of intense bands associated with partial oxidation species on ZrO_2 was not surprising, since according to the flow experiments, this catalyst showed a significantly low activity for the oxidation of DCE.

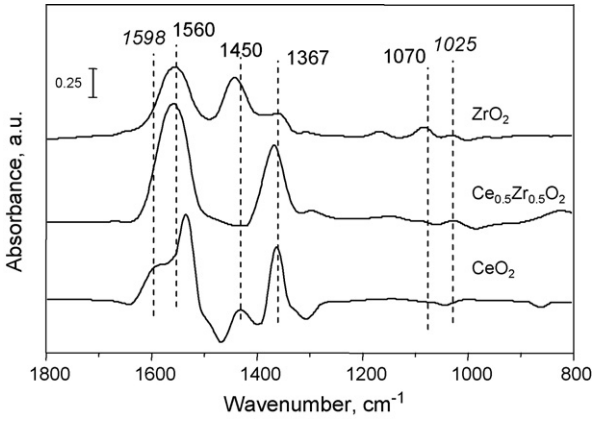

Fig. 8. Infrared spectra of DCE decomposition on $Ce_xZr_{1-x}O_2$ catalysts at 300 °C (1800–800 cm^{-1}).

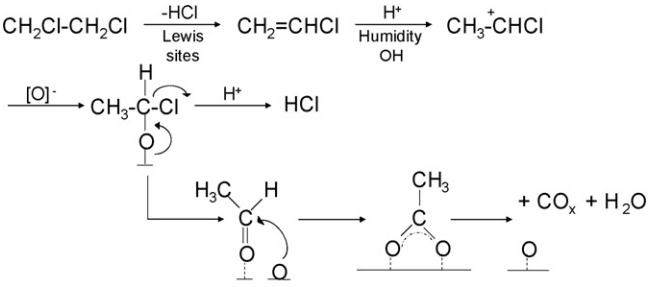

Fig. 9. Scheme of the DCE oxidation mechanism on $Ce_xZr_{1-x}O_2$ mixed oxides (adapted from Feijen-Jeurissen [15]).

When the spectra were collected in the absence of gas phase oxygen at the same temperatures, similar peaks were observed. This revealed that surface oxygen species of the catalysts reacted with adsorbed vinyl chloride to form the various adsorbed partial oxidation products. The intensity of these species, however, was lower in the absence of oxygen indicating further growth of these complexes in the presence of gaseous O_2.

The sequential presence with temperature of adsorbed species of DCE, VC, alkoxides, acetates, carbon dioxide and water was consistent with the mechanism proposed by Feijen-Jeurissen et al. [15] (shown in Fig. 9). This mechanism indicates that at low temperatures the DCE was first converted into VC mainly by the involvement of Lewis acid sites. This intermediate, detected in the flow experiments, would be protonated in presence of acid sites, moisture or OH surface species. By the protonation a reactive carbonium ion was formed, which could be attacked by nucleophilic oxygen species from the catalyst to generate adsorbed acetaldehyde. These species then would readily decompose to form surface acetate species, which finally were degraded into CO_x.

4. Conclusions

The surface reaction of 1,2-dichloroethane on ceria, zirconia and a number of ceria–zirconia mixed oxides with varying Ce/Zr molar ratio was investigated by means of a combined flow and infrared spectroscopic study with the aim of determining the ruling mechanism. It was shown that the catalytic conversion of the chlorinated compound required the participation of either acid and/or redox sites. Therefore, the mixed oxide with an optimum combination of both properties, $Ce_{0.5}Zr_{0.5}O_2$, led to a higher activity. The primary combustion products were CO_2, HCl and Cl_2. The yield of this latter undesired by-product (Cl_2) depended on the catalyst composition, and was significantly limited over zirconium-rich mixed oxide samples.

The in situ FTIR study carried out in the temperature range from 100 to 300 °C showed that DCE decomposition occurred via adsorption over acid sites and HCl removal to form vinyl chloride. The oxidation of this adsorbed intermediate was found to occur at the expense of lattice oxygen, resulting in the formation of various oxygen containing species such as alkoxide and acetates which were bound to the surface. The complexes underwent further oxidation at higher temperatures to yield complete oxidation products such as CO and CO_2.

Acknowledgements

The authors wish to thank UPV/EHU-Diputación Foral de Bizkaia (DIPE06/25) for the financial support of this work. One of the authors B. de Rivas acknowledges UPV/EHU for the post-doctoral financial aid.

References

[1] G. Centi, P. Ciambelli, S. Perathoner, P. Russo, Catal. Today 75 (2002) 3.
[2] C.S. Heneghan, G.J. Hutchings, S.H. Taylor, Catalysis 17 (2004) 105.
[3] H. Windawi, M. Wyatt, Platinum Met. Rev. 37 (1993) 186.
[4] K. Everaert, J. Baeyens, J. Hazard. Mater. 109 (2004) 113.
[5] S.C. Petrosius, R.S. Drago, V. Young, G.C. Grunewald, J. Am. Chem. Soc. 115 (1993) 6131.
[6] M.C. Álvarez-Galván, B. Pawelec, V.A. de la Peña O'Shea, J.L.G. Fierro, P.L. Arias, Appl. Catal. B 51 (2004) 83.
[7] A. Trovarelli, Catalysis by Ceria and Related Materials, Imperial College Press, London, 2002.
[8] A.C. Gluhoi, N. Bogdanchikova, B.E. Nieuwenhuys, J. Catal. 229 (2005) 154.
[9] J.R. González-Velasco, M.A. Gutiérrez-Ortiz, J.L. Marc, J.A. Botas, M.P. González-Marcos, G. Blanchard, Appl. Catal. B 22 (1999) 167.
[10] L.F. Liotta, A. Macaluso, A. Longo, G. Pantaleo, A. Martorana, G. Deganello, Appl. Catal. A 240 (2003) 295.
[11] W. Liu, M. Flytzani-Stephanopoulos, J. Catal. 153 (1995) 304.
[12] C. Li, Q. Xin, X. Guo, T. Onishi, Stud. Surf. Sci. Catal. 75 (1993) 1955.
[13] S. Scire, S. Minico, C. Cristafulli, C. Satriano, A. Pistone, Appl. Catal. B 40 (2003) 43.
[14] A. Setiabudi, J. Chen, G. Mul, M. Makkee, J.A. Moulijn, Appl. Catal. B 51 (2004) 9.
[15] M.M.R. Feijen-Jeurissen, J.J. Jorna, B.E. Nieuwenhuys, G. Sinquin, C. Petit, J.-P. Hindermann, Catal. Today 54 (1999) 65.
[16] P.S. Chintawar, H.L. Greene, J. Catal. 165 (1997) 12.
[17] S. Krishnamoorthy, M.D. Amiridis, Catal. Today 51 (1999) 203.
[18] R. López-Fonseca, A. Aranzabal, P. Steltenpohl, J.I. Gutiérrez-Ortiz, J.R. González-Velasco, Catal. Today 62 (2000) 367.
[19] J.I. Gutiérrez-Ortiz, B. de Rivas, R. López-Fonseca, J.R. González-Velasco, Appl. Catal. A 269 (2004) 147.
[20] B.M. Reddy, A. Khan, Y. Yamada, T. Kobayashi, S. Loridant, J.-C. Volta, J. Phys. Chem. B 107 (2003) 11475.
[21] M. Boaro, M. Vicario, C. de Leitenburg, G. Dolcetti, A. Trovarelli, Catal. Today 77 (2003) 407.
[22] G. Balducci, J. Kaspar, P. Fornasiero, M. Graziani, J. Phys. Chem. B 101 (1997) 1750.
[23] E. Finocchio, R.J. Willey, G. Busca, V. Lorenzelli, J. Chem. Soc., Faraday Trans. 93 (1997) 75.
[24] I. Hannus, Appl. Catal. A 189 (1999) 263.
[25] R. López-Fonseca, J.I. Gutiérrez-Ortiz, M.A. Gutiérrez-Ortiz, J.R. González-Velasco, Recent Res. Dev. Catal. 2 (2003) 51–75.
[26] R.W. van den Brink, P. Mulder, R. Louw, G. Sinquin, C. Petit, J.-P. Hindermann, J. Catal. 180 (1998) 153.
[27] T. Liu, T.I. Cheng, Catal. Today 26 (1995) 71.
[28] W.B. Feaver, J.A. Rossin, Catal. Today 54 (1999) 13.
[29] M. Tajima, M. Niwa, M. Fuji, Y. Koinuma, R. Aizawa, S. Kushiyama, K. Kobayashi, H. Mizuno, Ohuchi, Appl. Catal. B 12 (1997) 263.
[30] J.-Y. Miao, L.-F. Yang, J.-X. Cai, Surf. Interface Anal. 28 (1999) 123.
[31] G. Ranga Rao, H. Ranjan Sahu, Proc. Indian Acad. Chem. Sci. 113 (2001) 651.
[32] M.G. Cutrufello, I. Ferino, R. Monaci, E. Rombi, V. Solinas, Top. Catal. 19 (2002) 225.
[33] J.R. Sohn, S.G. Ryu, Catal. Lett. 74 (2001) 105.
[35] M.D. Driessen, T.M. Miller, V.H. Grassian, J. Mol. Catal. A 131 (1998) 149.
[36] M. Daturi, C. Binet, J.C. Lavalley, G. Blanchard, Surf. Interface Anal. 30 (2000) 273.
[37] M. Kang, J.H. Lee, S.-H. Lee, C.-H. Chung, K.J. Yoon, K. Ogino, S. Miyata, S.-J. Choung, J. Mol. Catal. A 193 (2003) 273.
[38] A. Yee, S.J. Morrison, H. Idriss, J. Catal. 186 (1999) 279.
[39] A. Yee, S.J. Morrison, H. Idriss, J. Catal. 191 (2000) 30.
[40] F. Ouyang, S. Yao, J. Phys. Chem. B 104 (2000) 11253.
[41] C. Li, Q. Xin, X.-X. Guo, Catal. Lett. 12 (1992) 297.
[42] E. Finocchio, G. Busca, V. Lorenzelli, R.J. Willey, J. Catal. 151 (1995) 204.

Further reading

[34] V.R. Choudhary, V.H. Rane, J. Catal. 130 (1991) 411.